Near-fields of Butterfly Nanoantenna Arrays: A Simulation Study

Saswatee Banerjee
Meta
Cork, Ireland
saswateeb@meta.com

Nicolas Marquez Peraca
Meta
Cork, Ireland
nmarquez@rice.edu

Alexander Franke
Meta
Cork, Ireland
alexfranke@meta.com

John Roberts
Meta
Cork, Ireland

***Abstract*—Optical nanoantennas demonstrate the ability to confine and enhance electromagnetic fields. This ability makes the nanoantennas essential tools for nano-optical devices and high-resolution microscopy. The response and resonances of the antennas are determined by the shape, size, material and the wavelength of light. In this paper we simulated the propagation and interaction of visible light with butterfly nanoantenna arrays using the finite-difference time-domain (FDTD) method. Experimental results measured on the same nanoantenna arrays by scanning near-field microscopy (SNOM) are reported in a separate paper.**

Keywords*—butterfly nanoantenna array, metallic projection (Fischer) pattern, near-fields, finite-difference time-domain method

I. Introduction

Interaction of light with metallic nanostructures are of great research interest. Such interactions give rise to surface waves or surface plasmon polaritons (SPPs) along the metal/dielectric interface. This makes subwavelength manipulation of the electromagnetic fields possible. Subwavelength confinement and enhancement of optical fields lead to various potential applications in integrated optics, such as coupling, waveguiding, sensing, high-resolution microscopy and so on. Nanoantennas in particular have been used near-field apertures that work as localized evanescent sources, effectively cutting the background illumination [1].

In this paper we consider the modelling and simulation of a plasmonic nanostructure (Fischer pattern) that consists of an array of butterfly nanoantennas. Our team also carried out an experimental investigation of a set of commercially available samples of metallic nanopatterns using scanning near-field optical microscopy (SNOM) [2]. The investigated samples consist of hexagonal periodic arrays of metallic butterfly nanoantennas deposited on a 0.15 mm-thick glass substrate [3].

The modelling and simulation of the Fischer pattern is carried out using the finite-difference time-domain (FDTD) method, the details of which is described in the following section.

II. FDTD Simulation of Fischer Pattern

A. Fischer pattern topography

Figure 1 shows the measured topography of two samples made from gold (Au, Fig. 1a) and aluminium (Al, Fig.1b) respectively. In both cases, the metallic nanoelements are arranged in a hexagonal array around a hole that serves as a transparent aperture. The approximate diameter d of the hole is 300nm for the Au and 1µm for the Al pattern respectively.

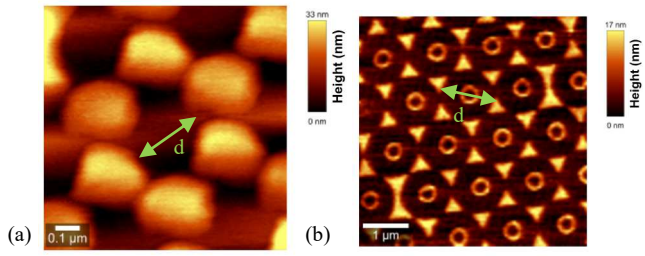

Fig. 1. Measured topography of the metallic (Fischer) nanoantenna pattern; (a) Au, (b) Al

B. Modelling and Simulation

To simulate the interaction of light with the sample in the near field, we created a computer model of a hexagonal arrangement of butterfly nanoantennas. Each butterfly nanoantenna consists of a pair of equilateral triangular elements. Two variants of the computer model that differ mainly from each other in the choice of the material of the nanoantennas and the inner aperture size, are simulated using FDTD. For the first variant of the computer model the material of nanoantennas is Au and the approximate diameter of the inner aperture is 400nm (Fig. 1a). In the second computer model the material of the nanoantennas is Al and the approximate diameter of the inner aperture is 1µm (Fig. 1b).

In the experimental set-up the illumination of the sample is achieved by laser light which is outcoupled through the SNOM tip aperture. In the simulation the illuminating source is modelled using an electric dipole [4].

The dispersive complex refractive indices for both Au and Al used in simulations here are obtained from published reference data [5]. Figure 2a shows the computer generated model with Au nanoantennas. A side of any of the nano triangle is ~200nm and the gap between the tips of the two adjacent triangles is ~25nm. The thickness of the nanotriangles is ~15nm.

The simulation of the computer generated models were carried out using the commercial FDTD package from Lumerical [5]. The spatial profile of the electric field intensity

978-1-7335096-3-3 ©2023 ACES

is computed for x and y orientations of the dipole respectively. Figure 2b shows the normalized electric field intensity computed at a wavelength of 532nm averaged over two orthogonal orientations of the dipole and recorded at 5nm from the surface of the structure.

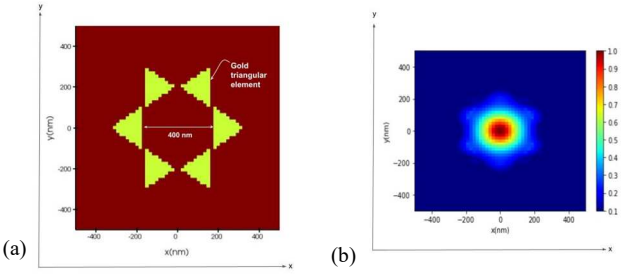

Fig. 2. (a) Computer generated model of the hexagonal arrangement of gold nano triangular elements, (b) xy-plane distribution of electric field intensity recorded at 5nm from the structure in 2a).

The electric field profile is also recorded at other distances from the surface of the structure by changing the position of the monitor along the z-axis. This is done to see how the field pattern changes as the distance from the surface of the structure increases. At each position of the monitor, the electric field profile is recorded for the two orthogonal in-plane polarizations of the dipole excitation source. Figure 3 shows the normalized electric field intensities averaged over the two orthogonal polarization states of the dipole recorded at distances 50nm and 100nm from the surface of the structure.

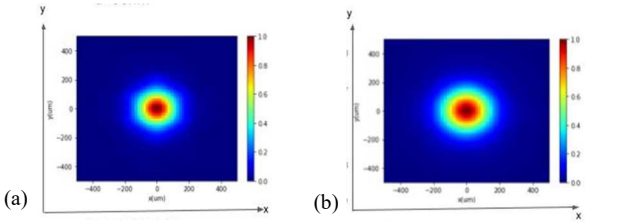

Fig. 3. Electric field intensity distribution in the xy-plane (a) 50nm, (b) 100nm from the surface of the structure in Fig. 2a

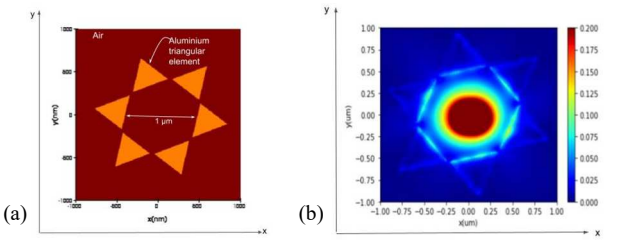

Fig. 4. (a) Computer generated model of the hexagonal arrangement of Al nano triangular elements, (b) xy-plane distribution of electric field intensity at a distance of 5nm along z-axis from the structure in 4a.

Figure 4a shows the second computer generated model of the hexagonal arrangement of Al triangular nanoantennas. The structure is rotated in the xy-plane by 20deg. Figure 4b shows the normalized electric field intensity computed at a wavelength of 532nm and averaged over two orthogonal polarization modes of the dipole and recorded at a distance of 5nm from the surface of the nanoantenna array.

III. RESULTS AND DISCUSSION

Light confinement is observed at a monitor distance less than 10 nm from the surface of the nanostructure (see Figure 2b, 3a and 3b). Confinement is also more prominent in any polarization state. Averaging over the two polarization states makes these confinements less obvious. However, at a distance less than 10nm the shape of the hexagonal aperture is more discernible. As the distance of the monitor is increased to $\lambda/2$ in intermediate steps of 50nm, 100nm and so on, the details disappear indicating that the light confinement seen in the near-field is due to evanescent waves that dissipate with increasing distance of the monitor from the surface of the nanostructure.

To be able to compare the simulated intensity maps with the SNOM measurements, the near-fields from the two polarization states were averaged in both Figures 2b and 4b, since the measurement system does not preserve the polarization state. In this case, the light confinement effects become less drastic, and the near- fields look more symmetric around the hexagonal aperture, which is similar to the experimental observations. Simulations in both cases involving Al and Au show that the triangular elements cast a shadow on the near-fields and light is only transmitted through the transparent aperture area in the centre. This result agrees with the experimental observation. Light confinement is seen to be stronger in case of the subwavelength aperture (d~400nm) in Fig.s 2b and 3.

ACKNOWLEDGMENT

The authors would like to thank Guillaume Lheureux, Yaniv Vinish and Shuyu Bao for useful discussions.

REFERENCES

[1] T. H. Taminiau, F. B. Segerink, R. J. Moerland, L (Kobus) Kuipers and N. F. van Hulst, "NEAR-FIELD DRIVING OF A OPTICAL MONOPOLE ANTENNA," Journal of Optics A: Pure and Applied Optics, vol. 9, no. 9, S315, April 2007.

[2] N. Marquez Peraca, S. Banerjee, J. Roberts, K.M. Kelchner, A. Franke, "Aperture-Based Scanning Near-Field Optical Microscopy of Metallic Projection Patterns," ACES 2023.

[3] Kentax UHV Equipment, "Projection pattern." Available at https://www.kentax.de/projection-pattern.html (11/1/2022).

[4] U. C. Fischer, J. Heimel, H-J. Maas, H. Fuchs, J. C. Weeber and A. Dereux, "Super-resolution scanning near-field optical microscopy," in Optical Nanotechnologies, Topics Appl. Phys. vol. 88, J. Tominaga and D.P. Tsai, Eds. Berlin Heidelberg: Springer-Verlag, 2003, pp. 141–153.

[5] Ansys Lumerical FDTD, https://www.ansys.com/en-gb/products/photonics/fdtd